
VARIOUS TECHNOLOGICAL PROCESSES

Kinetic and Thermodynamic Specific Features of Hydrogenation of Hexene-1, Heptene-1, and Cyclohexene on Catalyst Containing Copper Nanoparticles

R. V. Shafgulin*, N. S. Filimonov, E. O. Filippova, A. A. Shmelev, and A. V. Bulanova

Samara National Research University, Moskovskoe sh. 34, Samara, 443086 Russia

**e-mail: shafiro@mail.ru*

Received September 18, 2017

Abstract—Kinetics of hydrogenation of hexene-1, heptene-1, and cyclohexene on copper nanoparticles was studied. To examine the thermodynamic specific features, the entropy of formation of an activated complex, rate constants, and conversion were calculated. A conclusion that the key role is played by the entropy factor in the formation of the activated complex is made on the basis of the data obtained. The similarity between the mechanisms by which activated complexes are formed in the hydrogenation of hexene-1, heptene-1, and cyclohexene and in that of hexyne-1, hexadiene-1,5, and benzene with the use of nickel nanoparticles was confirmed. The results obtained enable a conclusion about the high catalytic activity of copper nanoparticles in reactions of hydrogenation of unsaturated hydrocarbons in the temperature range 140–200°C at a pressure of 2 atm.

DOI: 10.1134/S1070427217100147

The hydrogenation of unsaturated hydrocarbons is an industrially important process underlying the production of fuels that satisfy modern requirements to quality, polymers, and synthetic rubbers. The modernization of the existing technologies and the development of new effective, ecologically safe [1, 2], and economically more efficient technologies are the priority areas of modern science and economy [3, 4]. An important issue is in this case the development of inexpensive catalysts that are based on new materials and have an acceptable catalytic activity comparable with that exhibited by the catalysts presently used in industries [5, 6].

At present, researchers' attention is attracted by studies of the catalytic properties of nanomaterials [7–11] because nanostructures differ in properties from bulk materials. This is accounted for, in particular, by quantum-confinement effects changing the thermodynamic characteristics of chemical processes that involve these materials. Nickel catalysts are mostly industrially used for hydrogenation processes. The more inexpensive copper catalysts containing copper in the condensed state possess

a low catalytic activity in the hydrogenation processes because copper is inferior to nickel in absorption of hydrogen [6].

The goal of our study was to examine the catalytic activity exhibited by nanocatalysts containing copper nanoparticles in the hydrogenation of unsaturated hydrocarbons. The study is of both basic and applied nature. In the first case, thermodynamic features of these processes were examined to gain a deeper understanding of the heterogeneous catalysis on nanoparticles of transition metals. In the second, the process kinetics was analyzed to determine the catalytic activity of copper nanocatalysts in the hydrogenation of unsaturated hydrocarbons and the possibility of their industrial application.

EXPERIMENTAL

We used copper nanoparticles produced by the levitation-jet method at the Institute of Structural Macrokinetics and Materials Science Problems, Russian Academy of Sciences [12, 13]. The catalyst had the form

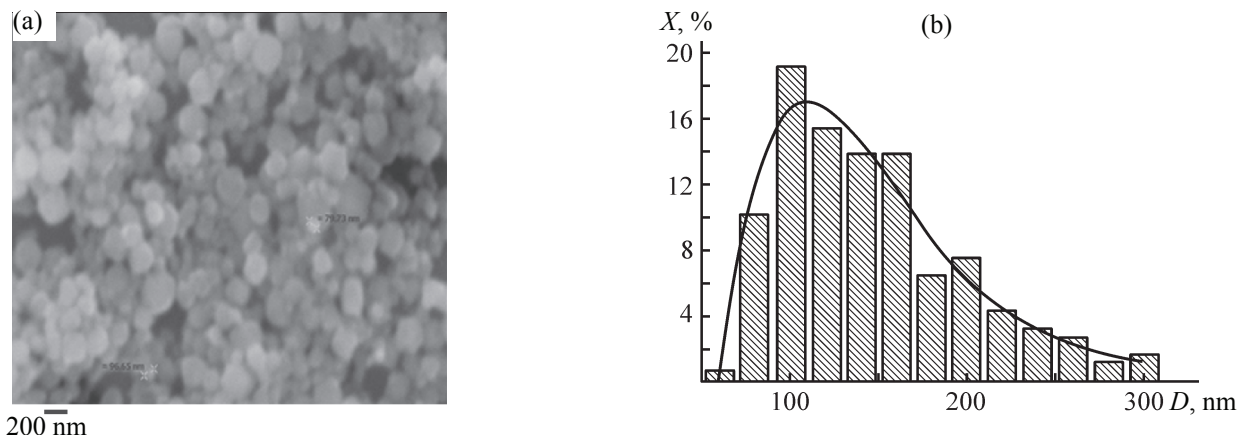


Fig. 1. (a) SEM image of copper nanoparticles and (b) particle size (D) distribution. (X) Number of particles.

of copper nanoparticles ultrasonically deposited from a colloid solution onto an inert support, INERTON NAW (Lachema BRNO, Praha, Czechoslovakia, with particle size 0.16–0.2 mm and specific surface area of $2 \text{ m}^2 \text{ g}^{-1}$). The mass fraction of copper nanoparticles was 15 wt %. The structure of the nanoparticles and the surface characteristics of the catalyst were examined by scanning electron microscopy (SEM) and by the method of low temperature adsorption-desorption of nitrogen. Figure 1 shows a micrograph of copper nanoparticles, obtained on a Carl Zeiss EVO 50 scanning electron microscope with an X-Max 80 energy-dispersive attachment, and the nanoparticle size distribution. The average particle size was 100 nm.

The specific surface area was found to be $1.2 \text{ m}^2 \text{ g}^{-1}$, which is quite reasonable for an inert nonporous surface, which is the surface of the INERTON NAW surface covered with metal nanoparticles [15].

The hydrogenation kinetics of hexene-1, heptene-1, and cyclohexene was studied on an original setup that enabled an on-line hydrogenation and analysis of the reaction mixture. The hydrogenation was performed at various temperatures and pressure of 2 atm. The setup is shown schematically in Fig. 2.

The setup is constituted by the reaction unit (thermostat with evaporator for introduction of liquid samples into the reactor) and analytical unit, a gas chromatograph. The units are connected with each other with a 6-port

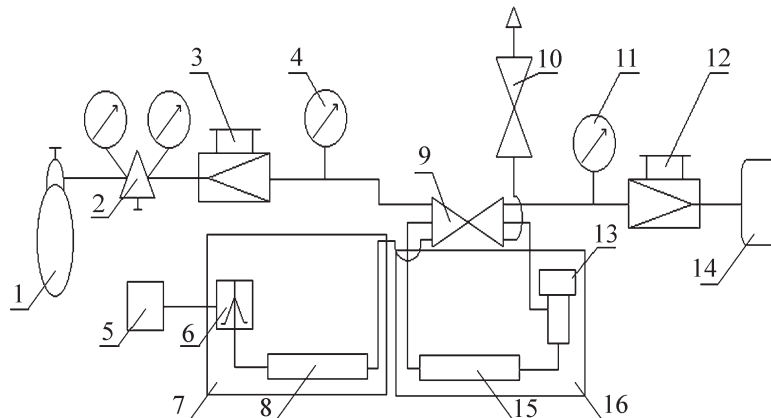


Fig. 2. Schematic of the setup for hydrogenation and analysis of the reaction mixture. (1) Cylinder with carrier gas, (2) reducing valve, (3) valve controlling the flow rate of the carrier gas, (4) gage measuring the pressure of the carrier gas in the analytical column, (5) computer and AD converter, (6) heat-conductivity detector, (7, 16) thermostats, (8) analytical column, (9) 6-port three-way valve, (10) valve at the hydrogen outlet from the reactor, (11) gage measuring the hydrogen pressure in the reactor, (12) hydrogen pressure reducer for delivery of hydrogen into the reactor, (13) evaporator (introduction of reagents into the reactor), (14) hydrogen generator, (15) reactor.

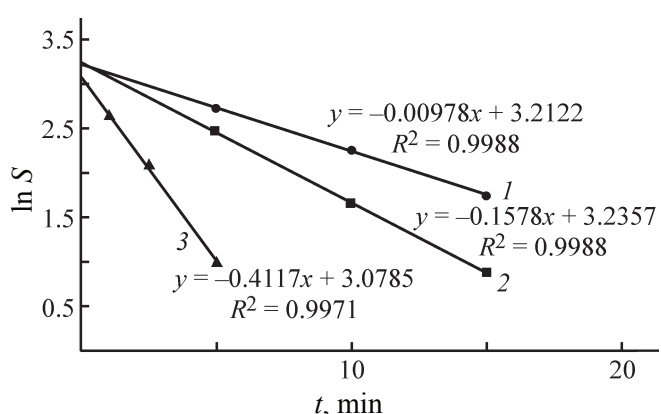


Fig. 3. Logarithm of the area under the peak, $\ln S$, vs. the duration t of the hydrogenation of heptene-1 at (1) 413.15, (2) 433.15, and (3) 453.15 K.

three-way injection valve. The loop in the injection valve is replaced with the reactor in which the gas-phase hydrogenation was performed. A hydrogen generator was used as a source of hydrogen. The hydrogen pressure in the reactor was monitored with a pressure gage. After certain intervals of time (the range of time intervals depended on the convenience of calculation), helium was passed through the reactor with the use of the 6-port three-way injection valve, and the reaction mixture was delivered into the analytical unit, the chromatographic column. The quantitative and qualitative compositions of the reaction mixture were determined from the chromatograms obtained. The qualitative and quantitative analyses of the reaction mixture were made with LKhM-80M gas chromatograph having a heat-conductivity detector. A system of two series-connected packed steel columns with Carbowax-20M (10%) and Carbowax-1,5M (10%) was used. Helium served as the carrier gas. The mixture was separated in the isothermal mode at 70°C. The chromatograms were processed with Mul'tikhrom 3.4.00121 software.

The reaction rate constant k was calculated from the kinetic equation of the first-order reaction because one of the reagents, hydrogen, was taken in a 16-fold excess. The rate constant was calculated from the peak areas of the starting reagent in the chromatograms of the reaction mixtures sampled from the reactor at certain intervals of time:

$$k = \frac{1}{t} \ln \frac{S_0}{S_t}, \quad (1)$$

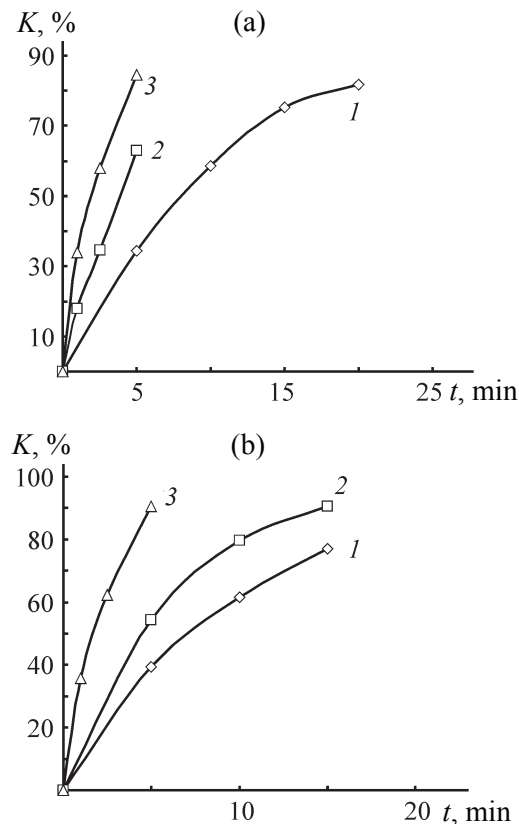


Fig. 4. Conversion K of (a) hexene-1 and (b) heptene-1 vs. the duration t of the hydrogenation reaction at (1) 413.15, (2) 433.15, and (3) 453.15 K.

where S_0 and S_t are the areas under reagent peaks at the initial instant of time and at the instant t after the beginning of the reaction, respectively.

The conversion K of the starting reagents was calculated by the formula

$$K = \left(1 - \frac{S_t}{S_0} \right) \times 100\%. \quad (2)$$

The activation energy of the reaction and the pre-exponential factor were found from the graphical dependence plotted in the coordinates of the Arrhenius equation ($\ln k - 1/T$).

To compare the mechanisms by which activated complexes are formed on the catalyst surface, the entropy of activation was calculated by the equation [15]:

$$\Delta S_p^\neq = R \ln \left(\frac{A h}{\chi k T e^x} \right) + (1-x) R \ln (RT), \quad (3)$$

where, A is the pre-exponential factor in the Arrhenius equation; R , gas constant; k , Boltzmann constant H , Plank constant; T , temperature; x , reaction molecularity; and χ , transmission factor.

RESULTS AND DISCUSSION

The hydrogenation reaction was performed in the static mode. Preliminarily, copper nanoparticles covered with an oxide film were reduced by passing hydrogen through the reactor at 330°C for 2 h. The kinetics of the reactions was examined by a chromatographic analysis of the reaction mixture, sampled from the reactor at certain intervals of time. The plots describing the dependence of the logarithms of areas under the peaks of hexene-1, heptene-1, and cyclohexene under study on the reaction duration are characterized by large values of the determination coefficient. Figure 3 shows a dependence of this kind for heptene-1 at three temperatures.

Similar dependences characterized by a good correlation were obtained for hexene-1 and cyclohexene.

The run of the dependences confirms the pseudo-first order of the reactions and, accordingly, the correctness of the results obtained. Table 1 lists the hydrogenation rate constants for hexene-1, heptene-1, and cyclohexene at three temperatures.

The conversion K of the unsaturated hydrocarbons under study was also calculated from the areas under their peaks in chromatograms of the reaction mixture in the initial instant of time and at a reaction duration t [Eq. (2)]. For the aliphatic hexene-1 and heptene-1, the maximum conversion was observed 5 min after the reaction onset at a temperature of 453 K, whereas for cyclohexene, it was observed in 60 min (Figs. 4 and 5).

With increasing temperature, the conversion steadily grows. It can be easily seen from the plots presented in these figures that the maximum conversion of cyclohexene is observed at a higher temperature, compared with hexene-1 and heptene-1, and the maximum conversion of cyclohexene is reached in a substantially longer time. This behavior is clearly illustrated by Fig. 6.

This fact is apparently related to the thermodynamic factors that cause the formation of the activated complex on the catalyst surface and to the activation energy of the reaction.

The dependence plotted in the coordinates of the Arrhenius equation, used to calculate the activation

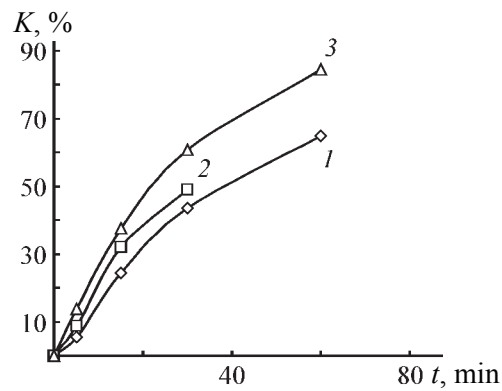


Fig. 5. Conversion K of cyclohexene vs. the duration t of the hydrogenation reaction at (1) 413.15, (2) 433.15, and (3) 453.15 K.

energy of the reaction of hexene-1 hydrogenation, is shown in Fig. 7.

Similar dependences were found for heptene-1 and cyclohexene, they all are characterized by large values of the determination factor.

It follows from the above data that the hydrogenation rate and the conversion of hexene-1 and heptene-1 exceed those of cyclohexene, whereas the activation energy of cyclohexene hydrogenation is lower. Hence, it can be suggested that, apparently, the thermodynamic factor governing the reaction rate is the entropy of activation, rather than the activation heat.

Table 1. Reaction rate constants for hydrogenation of the hydrocarbons under study at various temperatures and pressure of 2 atm

Reagent	T , K	k , min ⁻¹
Hexene-1	413	0.088
	433	0.201
	453	0.373
Heptene-1	413	0.098
	433	0.158
	453	0.412
Cyclohexene	433	0.017
	453	0.023
	473	0.031

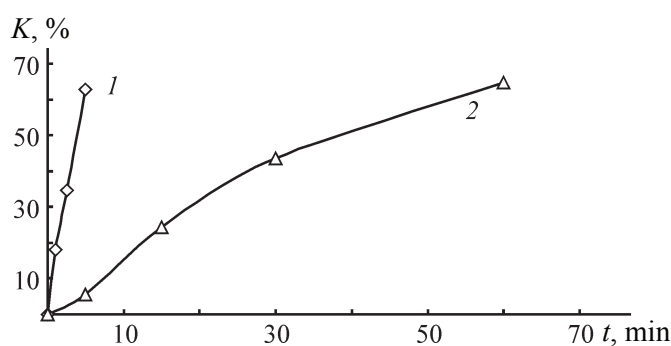


Fig. 6. Conversion K of (1) hexene-1 and (2) cyclohexene vs. the hydrogenation duration t .

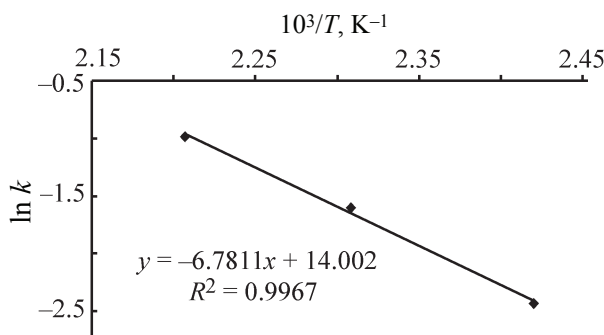


Fig. 7. Logarithm of the rate constant $\ln k$ of the hydrogenation of hexene-1 vs. inverse temperature $1/T$.

Equation (3) was used to calculate the entropies of activation, whose values are listed in Table 3.

In the general case, the reaction rate is determined not only by the activation heat, but also by the entropy of activation [15]. If the transition to the activated state leads to a strong rise in entropy, the reaction will occur at a higher rate, despite the high values of the activation energy. If, however, the entropy is low, the reaction will occur at a slower rate even at low activation energies. Thus, the smaller the absolute values of the entropy in the negative range, the higher the reaction rate. In this case, the entropy can be formally related to the steric factor. The values of the entropy of activation in Table 3 confirm the assumption of its key role in the formation of the activated complex: at a lower activation energy of the reaction of cyclohexene hydrogenation, compared with the activation energies for hexene-1 and heptene-1, the

hydrogenation rate constants of these latter exceed the constant of cyclohexene hydrogenation. Presumably the spatial orientation of hexene-1 and heptene-1 molecules relative to the catalyst surface is more favorable for the activated complex to be formed, compared with cyclohexene.

Previously the reactions of hydrogenation of hexyne-1 and hexadiene-1,5 on catalysts containing copper nanoparticles and of benzene on nickel nanoparticles with sizes of these latter of 20–60 and 50–200 nm have been studied [16–18]. An assumption was made in [6] that the formation of the activated complex in hydrogenation of unsaturated hydrocarbons on copper nanoparticles is due to the preliminary adsorption of hydrogen, its atomization, and subsequent interaction of hydrogen atoms with hydrocarbons at their multiple bonds. It was of interest to confirm this assumption that the mechanisms of the

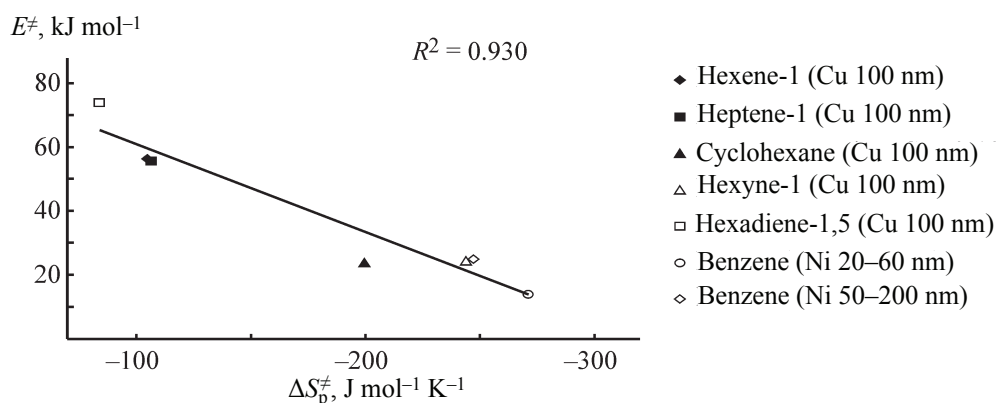


Fig. 8. Activation energy E^\ddagger vs. the entropy of activation, ΔS_p^\ddagger for the reactions of hydrogenation of selected unsaturated hydrocarbons and benzene on catalysts containing copper and nickel nanoparticles (NPs) ($T = 373$ K).

Table 2. Activation energies for the hydrogenation of the hydrocarbons under study

Hydrocarbon	Activation energy E^\ddagger , kJ mol ⁻¹
Hexene-1	56
Heptene-1	56
Cyclohexene	24

Table 3. Entropy of activation for the hydrogenation of the hydrocarbons under study

Hydrocarbon	Entropy of activation $-\Delta S_p^\ddagger$, J mol ⁻¹ K ⁻¹
Hexene-1	105
Heptene-1	107
Cyclohexene	200

reactions of hydrogenation of unsaturated hydrocarbons on copper and nickel nanoparticles are similar. The similarity of the reaction mechanisms is verified in an analysis of the isokinetic dependence described by the equation [19]:

$$\Delta H^\ddagger = \beta \Delta S^\ddagger, \quad (4)$$

where β is the compensation point (isokinetic temperature); ΔH^\ddagger , heat effect of the stage in which the activated complex is formed (in this study, we use the formation energy of the activated complex, E^\ddagger); and ΔS^\ddagger , entropy of activation.

The linear relationships between the energy-related component and the entropy are observed rather frequently, especially in those cases in which changes in the structure of compounds do not affect significantly the reaction center or these changes are sufficiently remote from the reaction center. Thus, it is assumed in the presence of a linear relationship that the reaction mechanisms are similar and independent of changes in the structure of starting substances, nature of a medium, and other factors. Figure 8 shows the compensation curve plotted in the coordinates $E^\ddagger - \Delta S_p^\ddagger$.

The existence of a linear correlation between the activation energy and entropy of activation ($R^2 = 0.930$), obtained on the basis of experimental data, suggests that the mechanisms of gas-phase hydrogenation of the

reagents under study on nickel and copper nanoparticles are similar.

CONCLUSIONS

(1) The kinetics and thermodynamic specific features of the reaction of hydrogenation of hexene-1, heptene-1, and cyclohexene on a catalyst containing copper nanoparticles with average size of 100 nm was studied. It was shown that the hydrogenation of aliphatic short-chain unsaturated hydrocarbons occurs at a higher rate than that of cyclohexene, with the entropy being the key thermodynamic factor governing the formation of an activated complex.

(2) It was found that the hydrogenation of the compounds under study on copper-containing catalysts is characterized by low activation energies at rather mild conditions of the process (temperature 140–200°C, pressure 2 atm): 56 kJ mol⁻¹ for hexene-1 and heptene-1 and 24 kJ mol⁻¹ for cyclohexene.

(3) The results obtained in the study suggest that development of catalysts base on copper nanoparticles is promising as regards their application in industrial processes for hydrogenation of unsaturated hydrocarbons.

ACKNOWLEDGMENTS

The study was supported by the Russian Foundation for Basic Research, grant nos. 15-43-02115 r_povolzh'e_a and 17-43-630358 r_a.

REFERENCES

- Mikhailova, I.V., Smolyagin, A.I., Krasikov, S.I., and Karaulov, A.V., *Immunologiya*, 2014, vol. 35, no. 1, pp. 51–55.
- Kon'kova, T.V., Katalevich, A.M., Gurikov, P.A., et al., *Sverkhkritich. Flyuidy: Teor. Prakt.*, 2013, vol. 8, no. 4, pp. 29–35.
- Thomas, S.P. and Greenhalgh, M.D., *Ref. Module Chem., Mol. Sci. Chem., Eng.*, 2014, vol. 8, pp. 564–604.
- Lakshmi Kantam, M., Kishore, R., Yadav, J., et al., *Ind. Catalytic Processes for Fine and Specialty Chemicals*, 2016, pp. 427–462.
- Obzor rynka promyshlennyykh katalizatorov v Rossii* (Review of the Industrial Catalyst Market in Russia), Moscow, 2010, 3rd ed. suppl. rev.
- Krylov, O.V., *Geterogennyi kataliz: uchebnoe posobie dlya vuzov* (Heterogeneous Catalysis: Textbook for Higher

- School, Moscow: Izd.-Knigotorg. Tsentr Akademkniga, 2004.
7. Zhu, L., Sun, H., Fu, H., et al., *Appl. Catal., A*, 2015, vol. 499, pp. 124–132.
 8. Crampton, A.S., Rötzer, M.D., Schweinberger, F.F., et al., *J. Catal.*, 2016, no. 333, pp. 51–58.
 9. Concepción, P., García, S., Hernández-Garrido, J.C., et al., *Catal. Today*, 2016, vol. 259, pp. 213–221.
 10. Kennedy, D.R., Jackson, S.D., and Lennon, D., *Appl. Catal., A*, 2004, vol. 259, pp. 109–120.
 11. Dokjampa, S., Rirksomboon, T., Osuwan, S., et al., *Catal. Today*, 2007, vol. 123, pp. 218–233.
 12. Ortega, D., Kuznetsov, M.V., and Morozov, Y.G., *J. Alloys Compd.*, 2013, vol. 579, pp. 495–501.
 13. Shishkovsky, I.V., Bulanova, A.V., and Morozov, Y.G., *J. Mater. Sci. Eng. B*, 2012, vol. 12, pp. 634–639.
 14. Ryzhonkov, D.I., Levina, V.V., and Dzidziguri, E.L., *Nanomaterialy* (Nanomaterials), Moscow: BINOM. Laboratoriya znanii, 2010, 2nd ed.
 15. Budanov, V.V., Lomova, T.N., and Rybkin, V.V., *Khimicheskaya kinetika* (Chemical Kinetics), St. Petersburg: Lan', 2014.
 16. Mitina, E.G., Shafigulin, R.V., Bulanova, A.V., and Shishkovskii, I.V., *Fizikokhim. Poverkhn. Zashch. Mater.*, 2014, vol. 50, no. 1, pp. 69–71.
 17. Shubina, E.G., Filimonov, N.S., Shafigulin, R.V., et al., *Sorbtionnye Khromatogr. Protsessy*, 2016, vol. 16, no. 5, pp. 701–710.
 18. Shubina, E.G., Filimonov, N.S., Shafigulin, R.V., et al., *Petroleum Chem.*, 2017, vol. 57, no. 5, pp. 410–414.
 19. Nakamura, K., Mizuta, R., Suganuma, S., et al., *Catal. Commun.*, 2017, vol. 102, pp. 103–107.